THE JOURNAL OF BIOLOGICAL CHEMISTRY
Vol. 275, No. 5, Issue of February 4, pp. 3522–3534, 2000

Printed in U.S.A.

Transcription Factor-dependent Loading of the E1 Initiator Reveals Modular Assembly of the Papillomavirus Origin Melting Complex*

(Received for publication, August 27, 1999, and in revised form, November 8, 1999)

Cyril M. Sanders and Arne Stenlund‡

From the Cold Spring Harbor Laboratory, Cold Spring Harbor, New York 11724

Replication of bovine papillomavirus type 1 DNA absolutely requires the viral transcription factor E2 as well as the initiator E1, although E1 alone has all the activities expected of an initiator protein. E1 assembles on the DNA in a stepwise fashion and undergoes a transition in activities from site-specific DNA-binding protein to mobile helicase. Complex assembly is assisted by the viral transcription factor E2 at two levels. E2 acts generally as a specificity factor, which through cooperative binding with E1 generates an initial E1 complex containing three E1 dimers bound to *ori* on one face of the DNA, E1-*ori*. Furthermore, E2 can promote the transition to an *ori* melting complex by recruiting additional E1 molecules to *ori,* effectively reducing the E1 concentration required for *ori* melting. This reaction is dependent on an E2-binding site positioned distal to the precursor E1-*ori* complex. The final origin melting complex has two subunits that each encircle the DNA and function independently to melt *ori*. The assembly pathway we describe has implication for understanding DNA melting and unwinding reactions, which are generally poorly understood.

Proteins that assemble on DNA in order to initiate replication and transcription must overcome two major obstacles. First, the size and sequence complexity of the genomes of higher organisms presents a significant challenge to correct start site selection by initiators, as nonspecific sites are in vast excess over specific sites. Recognition by the initiators of replication and transcription has been studied extensively. In many cases, these have limited sequence specificity, and targeting is achieved through cooperative binding mechanisms. The second obstacle arises from the double-stranded nature of DNA. In order to allow copying of the DNA, it must first undergo local denaturation or melting to allow access of enzymes and accessory factors. Subsequently, the DNA must then be unwound processively by a helicase as the DNA or RNA polymerase leaves the entry point (1). The protein factors involved in targeting, DNA melting, and processive unwinding may be distinct and form part of a multiprotein complex. Alternatively, a single protein may possess more than one of these activities.

DNA melting and unwinding reactions are poorly understood. In this respect, the initiators of DNA replication in eucaryotic DNA tumor viruses are an important class of protein. These have all the activities required for initiation, including origin recognition and melting, and also act as DNA helicases (2–5). They also provide a fascinating example of how a single protein can undergo a transition in activities that, paradoxically, appear to be incompatible. For example, site-specific DNA binding and helical motor activity could be considered to be mutually exclusive properties. The initiator protein E1 of the bovine papillomavirus BPV-1[1] is also unique in another respect. The ability of E1 to initiate replication *in vivo* is absolutely dependent on the viral transcription factor E2, which appears to act as a loading factor for the viral helicase (6, 7).

E1 and E2 are the only viral proteins required for initiation of BPV-1 replication *in vivo,* and binding sites for both, as well as an A/T-rich region, are found in the replicator. Although absolutely required, there is flexibility in terms of the positioning of the E2 site relative to the E1-binding site. In general, as the spacing between the two sites is increased, higher affinity or multiple E2-binding sites are required (8, 9). We have extensively characterized a replicator with proximal E1- and E2-binding sites (E2 BS12) separated by 3 base pairs (7, 10–13). On this origin, E2 stimulates formation of an E1-*ori* complex active for *ori* melting in at least two steps. First, a highly sequence-specific E1E2-*ori* complex forms, and then additional E1 molecules are recruited and E2 is displaced. The second step is ATP-dependent, resulting in deposition of a complex with low sequence specificity at a specific site (7). Similar results have been obtained by others (6). In the viral genome, a second E2-binding site distal to the E1-binding site (BS11) may have a role in formation of an active replication complex (14, 15). This activity has also been observed for the cellular transcription factor AP-1, which interacts directly with polyomavirus large T, stimulates its binding to *ori,* and activates replication (16).

Here we have extended our studies on the role of E2 in BPV-1 initiator complex assembly. The origin melting complex, in which the DNA is denatured immediately upstream and downstream of the E1-binding site, forms through a number of intermediates. In the first E1 complex that forms on the origin, six E1 molecules contact the DNA, the DNA lies on a protein surface, and the protein wraps extensively around the DNA. This complex is the immediate product of the E2 loading cycle from proximal E2 BS12 and forms the core or nucleus of the higher order origin melting complex. E2 bound to distal binding sites can recruit additional E1 molecules to this precursor complex, preferentially melting the origin DNA nearest the E2 site. Thus, the origin melting complex is composed of two functional subunits that form through a common precursor. The results are discussed in terms of other known proteins that melt and unwind DNA.

* This work was supported by National Institutes of Health Grant CA 13106 (to A. S.) and in part by a Wellcome International Prize Travelling Fellowship (to C. M. S.). The costs of publication of this article were defrayed in part by the payment of page charges. This article must therefore be hereby marked "*advertisement*" in accordance with 18 U.S.C. Section 1734 solely to indicate this fact.

‡ To whom correspondence should be addressed: Cold Spring Harbor Laboratory, P. O. Box 100, Cold Spring Harbor, New York, NY 11724. Tel.: 516-367-8407; Fax: 516-367-8454; E-mail: Stenlund@cshl.org.

[1] The abbreviations used are: BPV-1, bovine papillomavirus type 1; BS, binding site; AD, activation domain; DBD, DNA binding domain; EtBr, ethidium bromide; bp, base pair; oligo, oligonucleotide; SSB, single-stranded-binding protein.

MATERIALS AND METHODS

Viral Proteins and Origin Templates—Production of E1 and E2 and the anti-E2 antibody have been described previously (7, 12). Origin templates were based on a 110-base pair BPV-1 sequence (nucleotides 7894 to 57, centered about the E1-binding site) cloned between the *Xba*I and *Hin*dIII sites of pUC19. This sequence encompasses the two native BPV-1 E2-binding sites BS11, 33 bp upstream of the E1-binding site, and BS12 immediately downstream (3-bp separation) of the E1 site. The A/T-rich region (A/T) is between BS11 and the E1-binding site. In some constructs, an E2-binding site was placed 33 bp downstream of the E1-binding site, a symmetrical transposition of upstream BS11. The sequence of the E2 sites in various constructs was changed to alter the affinity of the E2 protein. The nomenclature used is based on the prototype wild type template 11/12/X, where 11 indicates upstream BS11, 12 is the site immediately adjacent to the E1-binding site, and X indicates no site engineered at the distal downstream position. Substitutions of upstream BS11 were AACCATCACCGTTTT (BS12) or CCAGAACACTGG to mutate BS11 (site X). The sequence GTCATACCCACT was substituted for BS12 at the native position to mutate this site. For constructs with E2 sites downstream, the 12-bp BPV sequence from nucleotides 46 to 57 was substituted for ACCGAAACCGGT (BS11), AACCTAAACGGT (BS16), or *GTC*ATCCAC*ACT* (mutant site X). In construct 12/X/16, 13 base pairs of the pUC19 polylinker were deleted by cleavage with *Eco*RI and *Bam*HI and religation after Klenow treatment. For some hydroxyl radical footprinting (Fig. 6), the E2 site of E2 BS12 was modified to ACCAT**GG**CCGTT, generating a *Hae*III restriction site. For hydroxyl radical footprinting of E2 bound to BS9, the template comprised BPV nucleotides 7894 to 27 with E2 BS12 substituted for ACCGTTGCCGGT (BS9). The affinity of E2 for the various binding sites in the BPV-1 genome has been described in detail (17). BS9 is a high affinity site, with a relative affinity approximately 5-fold greater than BS11, 10-fold greater than BS16, and 50-fold greater than BS12.

DNA Binding Assays—Probes were generated by polymerase chain reaction using one ^{32}P-end-labeled primer from the pUC19 polylinker (upstream 5′-GTAAAACGACGGCCAGT and downstream 5′-GGATAACAATTTCACACAGG). For biotinylated probes, one primer was labeled at the 5′ end with biotin. Binding buffer was 20 mM $NaPO_4$ (pH 7.2), 100 mM NaCl, 1 mM EDTA, 0.1% Nonidet P-40, 1 mM dithiothreitol, 10% (v/v) glycerol, 0.1 mg/ml bovine serum albumin, 125 pg/μl poly(dA-dT)$_n$, and 5 mM ATP/$MgCl_2$ (unless otherwise stated). The probe concentration was 0.025 to 0.1 nM as indicated, and reactions were incubated for 50 min at 20–22 °C. Complexes were cross-linked with 0.08% glutaraldehyde, and the reaction was quenched with Tris-HCl (pH 7.5) added to 80 mM after 5 min. When complexes were analyzed in the presence of EtBr it was added to 25 μg/ml for cross-linked complexes and 4 μg/ml without cross-linking. The short competitor oligonucleotides were BS9 5′-ACAAGTACCGTTGCCGGTCGGGGTC and the corresponding mutant 5′-ACAAGTCACGTTGCCGTGCGGGGTC. The sequence of BS10 was 5′-CTTAAACCGTCTTCGGTGCAAACCGTCTTCGGTGCGGT, and the mutant, 5′-CTTAAGGCGTCTTCACTGCAAGGCGTCTTCACTGCGGT. After electrophoresis, binding reactions were quantified using phosphorimaging technology (Fuji Bas 1000).

Potassium Permanganate Modification Assay—Each probe was at 0.025 nM. If the concentration of Mg^{2+} (or other divalent ions) is increased during $KMnO_4$ modification, the extent of modification at high E1 concentrations increases such that 80% or more of the input template can be modified at at least one position.[2] For maximum reactivity (as in Fig. 5), reactions (200–400 μl) were treated with an equal volume of 55 mM $MgCl_2$, 100 mM NaCl, 10% glycerol, and 12 mM $KMnO_4$ for 2 min before quenching. $KMnO_4$ was added to the solution immediately before use. Otherwise, the concentration of $MgCl_2$ in the 2× solution was 25 mM. Reactions were processed as described previously, and products were analyzed on 8% urea-acrylamide gels (7).

DNase I Footprinting—DNase I footprinting in solution was performed as described previously (7). When biotinylated probes were used, digestion was terminated with 20 mM EDTA, and the products of nuclease cleavage were selectively recovered by binding to streptavidin-agarose (Sigma; 20 μl for 1.5 ml of solution) for 1 h. Beads were washed 4 times (~5 min) with 1 ml of wash buffer (200 mM NaCl, 1 mM EDTA, pH 8.0, 0.1% SDS). DNA was eluted by heating to 97 °C in 100% formamide (2 × 75 μl) for 10 min, mixed with an equal volume of 600 mM NH_4Ac, 0.05% SDS, 1 mM EDTA, phenol/chloroform extracted and precipitated with ethanol. Scission products were analyzed as above.

Hydroxyl Radical Footprinting—The general guidelines of Dixon *et al*. (18) were observed. Probe was at 0.1 nM and reactions contained no glycerol. The hydroxyl radical was generated by addition of 1 mM sodium ascorbate, 0.075% (w/v) H_2O_2, 4 mM [$(NH_4)_2Fe(SO_4)_2{\cdot}6H_2O$], 8 mM EDTA for 2 min. Reactions were quenched with 0.5 volume of 200 mM thiourea, 25% v/v glycerol, 20 mM EDTA, 2% SDS, and 0.15 μg/μl carrier DNA. Cleavage products were recovered and analyzed as described above. For footprinting of complexes immobilized on streptavidin-agarose, biotinylated probe was bound to beads (0.5- or 1-ml reactions, 10- or 20-μl beads) for 40 min after complex formation. Beads were recovered by centrifugation, and the supernatant was removed to leave 100 μl of the binding reaction. 5 μl of 100 mM $MgCl_2$ and 100–200 units of restriction enzyme (*Mse*I or *Hae*III) were added, and the DNA was digested for 8 min at room temperature. For footprinting all complexes other than E1E2-*ori*, EtBr was added to 4 μg/ml halfway through the incubation with enzyme. After digestion, beads were recovered, washed rapidly in binding buffer without glycerol (twice), and resuspended in binding buffer (0.4× the original reaction volume). The hydroxyl radical cleavage reaction was performed as above. Beads were washed four times in 200 mM NaCl, 1 mM EDTA pH 8.0, 0.1% SDS, 25% glycerol, and the DNA eluted from the beads into 100% formamide as described above.

RESULTS

E2-dependent E1-ori Formation from Proximal and Distal E2-binding Sites—At low E1 concentration in the presence of E2, an E1E2-*ori* complex forms with high sequence specificity and affinity and is a precursor for formation of a multimeric E1-*ori* complex. As a targeting and assembly factor, E2 lowers the concentration of E1 required for E1-*ori* formation *in vitro*. However, the *in vitro* origin melting activity of the E1-*ori* complex that formed from E1E2-*ori* was low, compared with an E1-origin complex formed at higher E1 concentrations without E2 (7). Accordingly, we have further examined E1-*ori* complex formation and activity, including the action of a second E2 site, E2 BS11, found 33 bases upstream of the E1-binding site in the viral DNA. We investigated E1-*ori* complex formation *in vitro*, with and without E2, on origins with both proximal E2 BS12 and distal BS11.

Complexes formed in the presence of ATP/Mg^{2+} were analyzed by gel shift assay after glutaraldehyde cross-linking (Fig. 1*A*). The binding site configuration of each probe is shown next to each autoradiograph, as in all subsequent figures. Here, the E1-binding site is represented by the *arrows*. For the origin with both E2 sites, *ori* 11/12/X (see the note on probe nomenclature under "Viral Proteins and Origin Templates" under "Materials and Methods"), E2 stimulated E1-*ori* complex formation at low E1 concentration (Fig. 1*A, lane 3* compared with *lanes 4–7*). The resulting complex co-migrates with the E1-*ori* complex formed at high E1 concentration (*lane 2*), and binding of E2 alone could not be detected (*lane 8*). An E2-binding site oligonucleotide (*BS9*), but not a mutant sequence (*MUT*), inhibited complex formation (*lanes 9* and *10*), demonstrating the need for E2 binding. The template lacking BS11 (X/12/X) behaved similarly, but at the same E1 concentration complex formation was reduced (*panel immediately below*). Most of the products of reaction 7 (*lane 7*) with probe 11/12/X could be supershifted with anti-E2 antibody (*lane 13, top panel*). In contrast, E2 is displaced from E1-*ori* during loading from proximal E2 BS12 (*lane 13*, *panel immediately below*). In *lanes 16–18* the products of reaction 7 were challenged with either E2 BS9 oligo, mutant E2 oligo competitor or buffer, and incubated for a further 30 min before cross-linking. Addition of anti-E2 antibody revealed that E2 is free to dissociate from the complex that forms on *ori* 11/12/X, whereas E1-*ori per se* is stable (*lane 16*). Almost identical result were obtained on the origin with only distal E2 BS11 (ori 11/X/X), indicating minimal cooperation between the two E2-binding sites (*3rd panel* from *top*). All E2 sites tested functioned from the distal position, including low affinity E2 BS12 (12/X/X, *bottom panel*). This analysis also revealed that E2 dissociates from E1-*ori* at a rate

[2] C. M. Sanders and A. Stenlund, unpublished observations.

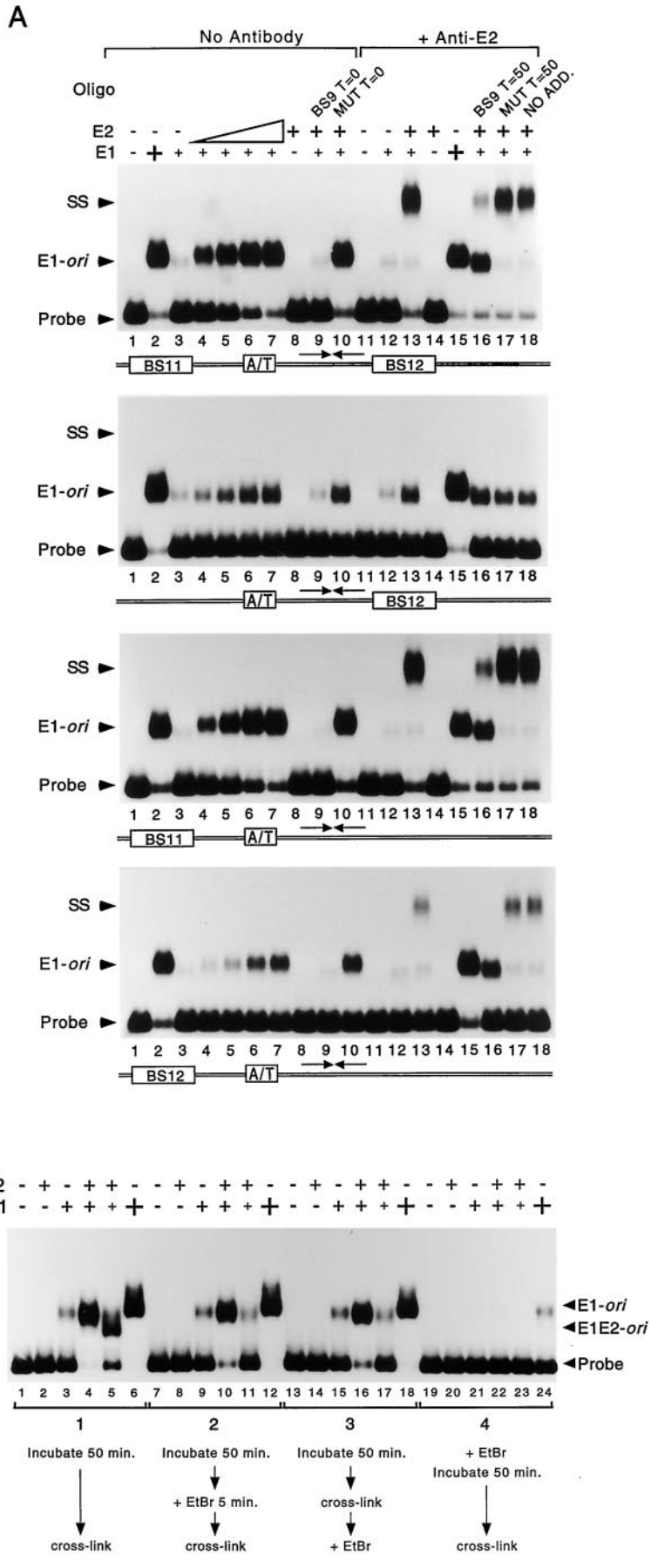

FIG. 1. *A,* E2-dependent E1-*ori* formation from proximal and distal E2-binding sites. Reactions contained ATP/Mg^{2+} and the following probes (0.05 nM) from *top* to *bottom*: 11/12/X (wild type), X/12/X, 11/X/X, and 12/X/X. Products were analyzed in the presence of EtBr. *Lane 1*, free probe, and *lane 2*, high E1 concentration (37.5 nM). In reactions (*lanes 3–7*), E1 was at 7.5 nM. *Lane 3*, no E2; *lanes 4–8*, E2 at 0.125, 0.25, 0.5, 0.75, and 0.75 nM. In reactions 9 and 10, E1 was at 7.5 nM, and E2 was at 0.75 nM. E2 BS9 oligonucleotide (180 nM), but not a mutant sequence, inhibited complex formation (*lanes 9* and *10*). In *lanes 11–15*, the products of reactions 1, 3, 7, 8, and 2 were analyzed with anti-E2 antibody (*SS* = supershift). In *lanes 16–18*, the products of reaction 7 were challenged for 30 min with E2 BS9 oligo, mutant oligo, or buffer before cross-linking and analysis with anti-E2 antibody. *B,* stability of E1-*ori* and E1E2-*ori* in the presence of EtBr. The probe used was X/12/X, native proximal E2 BS12 only. Reaction 1 (*lanes 1, 7, 13,* and *19*), free probe; 2 (*lanes 2, 8, 14,* and *20*), E2 2 nM; 3 (*lanes 3, 9, 15,* and *21*), E1 15 nM; 4 (*lanes 4, 10, 16,* and *22*), E1 15 nM and E2 2 nM; 5 (*lanes 5, 11, 17,* and *23*), E1 4 nM and E2 2 nM; 6 (*lanes 6, 12, 18,* and *24*), E1 50 nM. Reactions were treated as indicated.

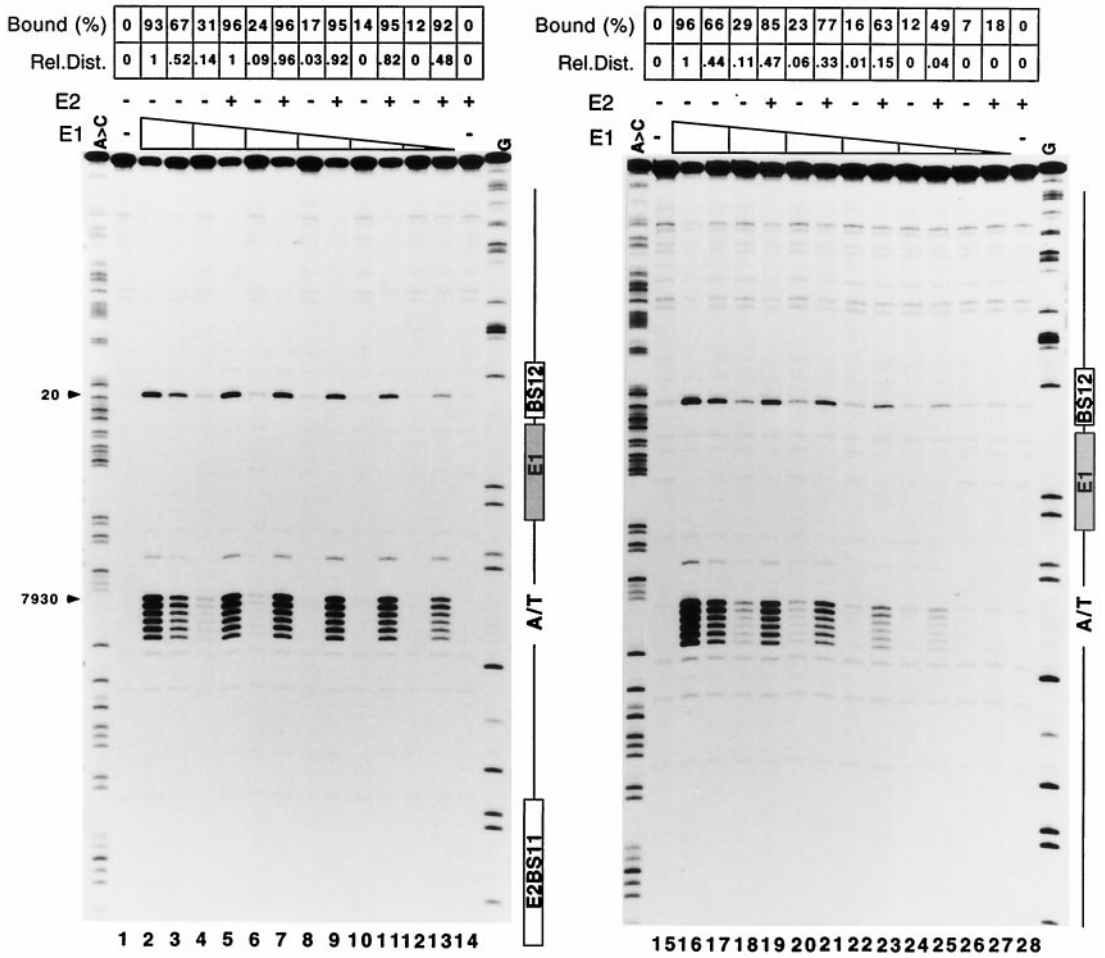

FIG. 2. ***ori* melting with proximal and distal E2-binding sites.** Probes labeled on the *top strand* 11/12/X (*left*) and X/12/X (*right*) were analyzed by gel shift and the $KMnO_4$ assay. Where added, E2 was at 1.5 nM. *Lane 1*, reactivity of free probe. *Lanes 2* and *3*, E1 at 90 and 50 nM. *Lanes 4* and *5*, E1 at 30 nM; *lanes 6* and *7*, 25 nM; and *lanes 12* and *13*, 5 nM E1. Protein concentrations for reactions 15–28 were as *lanes 1–14.* Major reactive residues are indicated (*left*) for each origin shown *right* of each panel. A > C and G are chemical sequence ladders of probe 11/12/X. The figures *above* each lane are the fraction of probe bound (*Bound (%)*) and a relative measure of *ori* melting or distortion (*Rel.Dist.*) compared with reaction 2 or 16.

proportional to the affinity of the E2-binding site (compare *lanes 16–18, bottom two panels* and data not shown), indicating that E2 DNA binding is a component of the interactions that stabilize its association with E1-*ori*. All origins replicated *in vivo* (not shown). Thus, E2 stimulates E1-*ori* formation *in vitro* from proximal or distal E2 sites, but active displacement of E2 occurs only from proximal BS12. We have termed origins with an E2-binding site proximal to the E1-binding site (as BS12) type I origins and any with a distal site type II origins.

In E1-*ori,* E1 molecules encircle the DNA, but in E1E2-*ori* the proteins are bound to one face of the DNA helix (11). The cross-linked E1-*ori* complex, but not the E1E2-*ori* complex, is stable in the presence of the intercalator ethidium bromide (EtBr, 25 μg/ml), which disrupts protein-DNA but not protein-protein interactions. We suggested that in the E1-*ori* complex the DNA is inaccessible to EtBr compared with E1E2-*ori*. (7). We have now observed the same sensitivity of the complexes to EtBr, regardless of prior glutaraldehyde cross-linking.

In Fig. 1*B*, binding reactions with probe X/12/X were assembled (with ATP/Mg^{2+}) to generate the E1E2-*ori* complex (*lane 5*), the E1-*ori* complex at low and high E1 concentrations independently of E2 (*lanes 3* and *6* respectively), and at low E1 concentration in the presence of E2 (*lane 4*). When treated with EtBr before cross-linking (*lanes 7–12*), the E1-*ori* complex was largely insensitive to the intercalator (*lanes 9, 10,* and *12*), but the E1E2-*ori* complex dissociated completely (*lane 11*), even though the time elapsed before cross-linking (5 min) was less than the half-life of the E1E2-*ori* complex (~35 min). The expected result was observed when complexes were treated with EtBr after cross-linking (*lanes 13–18*). Addition of EtBr before the proteins abolished most complex formation at all but the highest concentration of E1 (*lane 24*). Therefore, accessibility of DNA-binding sites appears to be a good explanation to account for the relative sensitivities of the origin complexes to EtBr.

E2 Reduces the E1 Concentration Required to Generate an Ori Melting Complex—The probes analyzed for E1 binding in Fig. 1*A* were also tested for DNA melting over a range of E1 concentrations, with or without E2. A sample of each reaction was treated with $KMnO_4$ which reacts with T residues in single-stranded or distorted DNA (19). The results are shown in Fig. 2, for *ori* 11/12/X (*left*) and X/12/X (*right*). A measure of relative *ori* melting (*Rel.Dist.*) was obtained by comparing the extent of $KMnO_4$ reactive products in each reaction to those generated at the highest concentration of E1 where practically all the probe was bound, and melting was maximal (reactions 2 and 16, *lanes 2* and *16*). Gel shift analysis was used to determine site occupancy (*Bound %*). Gel shift and DNase I footprinting give identical results for site occupancy over the full range of E1 concentrations and binding extents (data not shown). Thus, each assay is likely to give an accurate measure of this parameter.

Without E2 the extent of E1-*ori* complex formation and *ori* melting activity are the same for all the probes (compare *% bound* and *Rel.Dist.* for reactions 2–4, probe 11/12/X (*lanes 2–4*), with the corresponding reactions in *lanes 16–18*, probe X/12/X, Fig. 2). In addition, the *ori* melting activity of the E1-*ori* complex that forms independently of E2 at low E1 concentrations is low. For example, compare *% bound* and *Rel.Dist.* in reactions *lane 10* (probe 11/12/X) and *lane 24* (probe X/12/X); 14 and 12% of the probe was bound in each case, but *ori* melting was practically undetectable. Finally, E2 stimulates formation of an E1-*ori* complex on both probes, but E2 from distal E2 BS11 is more efficient in stimulating *ori* melting. For example, in reaction 11, where E2 stimulated E1-*ori* formation on probe 11/12/X, 95% of the probe was bound, and melting was 82% relative to the reference. At the same E1 concentration in reaction 25, where E1 was loaded from E2 BS12, 49% of the probe was bound, but only 4% of templates were melted, relative to the reference. This translates into a significant difference in specific activity, greater than 10-fold. E2 at a distal site fails to generate a complex with high *ori* melting activity on type II origins only when E1 can be considered to be limiting, compare *lanes 2* and *13*. Complex formation is similar in each case but, where E2 stimulated E1-*ori* formation at very low E1 concentration (reaction 13) *ori* melting (*Rel.Dist.*) is lower.

Therefore, formation of a melting complex is proportional to the E1 concentration, and two types of E1-*ori* complex can form. A complex with low or no melting activity forms at low E1 concentration and is also the immediate product of the E2 loading cycle from proximal E2 BS12 (type I *ori*). A complex with high *ori* melting activity forms at high E1 concentration or at low E1 concentration in the presence of E2 on origins with a distal E2-binding site (type II *ori*). A distribution of differently sized E1 complexes with different numbers of E1 molecules could account for these observations. Only when the protein concentration is high, and the vast majority of the probe is bound, are all the E1 molecules required for melting activity bound in the E1-*ori* complex. The notion that a minimal core E1-*ori* complex (inactive for *ori* melting) appears at low E1 concentration is supported by our observations that glutaraldehyde cross-linking may stabilize only a subset of E1 molecules bound to *ori* and that different DNase I footprints are generated at high and low E1 concentrations (7).[2] These ideas are summarized in the model shown in Fig. 3.

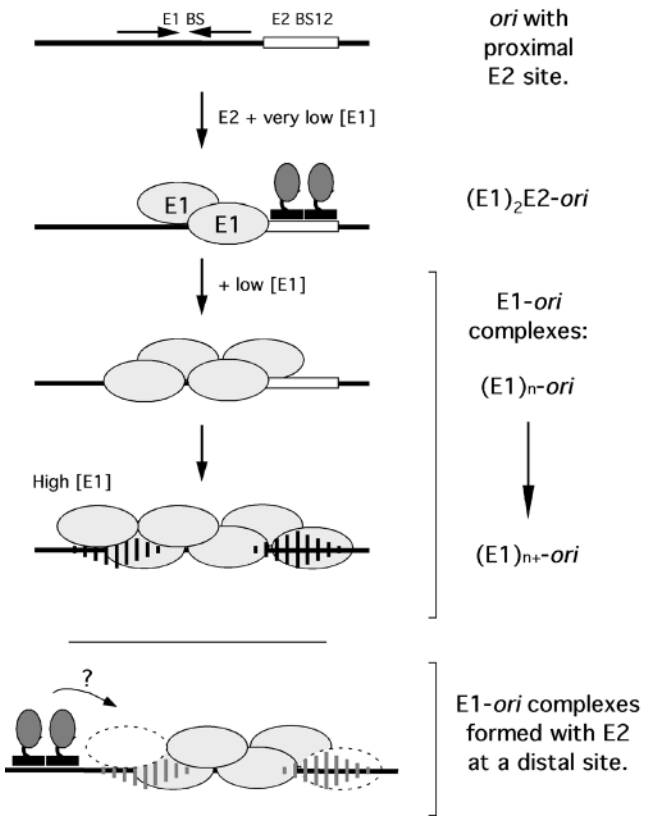

FIG. 3. **Assembly of the E1 origin melting complex.** E1E2-*ori* is a dimer of E1 and E2 bound to proximal E1 and E2 (BS12)-binding sites (13). This complex can be converted to $(E1)_n$-*ori* at elevated E1 concentrations in the presence of ATP. The number of E1 molecules in this complex is unclear. The *ori* melting by this complex is low compared with one that forms at high E1 concentrations without E2. DNase I footprints of E1-origin complexes that form at low E1 concentration with and without ATP or via E2 are all similar, with complete protection over the E1-binding site and partial protection of the flanking sequences. At high E1 concentration the flanking sequences become completely protected. We have suggested that this complex ($(E1)_{n+}$-*ori*) may be related to $(E1)_n$-*ori* by addition of E1 molecules (7). Here we have further characterized these origin complexes. To assist, we have analyzed the activity of E2 at distal sites. E2 may affect the activity of E1-*ori* or could generate a higher order *ori* melting complex.

E1 Loaded from a Distal E2 Site Preferentially Melts the DNA Adjacent to the E2-binding Site—Close examination of Fig. 2 revealed that on type II origins in the presence of E2, $KMnO_4$ reactivity is biased toward the region adjacent to the E2-binding site. For example, the scission products in the A/T-rich region and at residue 20 in reactions with E1 only (*lanes 2*-4, *6,* and *8* and so on) decrease proportionally as protein concentration and complex formation decrease. This is also seen on *ori* X/12/X, regardless of whether complex formation is stimulated by E2 (*lanes 16–27*). However, when E2 stimulated complex formation at low E1 concentrations on probe 11/12/X (*lane 13*), residue 20 is less reactive than those in the A/T-rich region compared with reaction 2 (*lane 2*), where the extent of complex formation was similar. This was investigated further by comparing an origin with E2 BS11 symmetrically transposed to a position downstream of the E1-binding site (*ori* X/X/11) with *ori* 11/X/X. Binding reactions were assembled and analyzed as in Fig. 2.

Fig. 4, *lanes 2–6*, and *8, 10, 12*, and *14* (*left*) and *18–22*, and *24, 26, 28,* and *30* (right) show $KMnO_4$ reactivity (bottom strand labeled) with decreasing E1 for origins 11/X/X and X/X/11, respectively. As above, $KMnO_4$ reactivity on either side of the E1-binding site decreases proportionally with complex formation (*Bound %*) on both probes. In contrast, where E2 stimulates E1-*ori* formation at low E1 concentrations (*lanes 7, 9, 11, 13,* and *15*, probe 11/X/X *left,* and 23, 25, 27, 29, 31, probe X/X/11 *right*), *ori* melting is asymmetric, preferentially occurring adjacent to the E2 site. For example, in reaction 9 (*lane 9*), where E1-*ori* was formed with E2, the A/T-rich region is hyperreactive and the downstream region (around residue 19) hyporeactive, compared with *lane 3* where the E1-*ori* complex was formed at high E1 concentration. Importantly, when the E2-binding site is moved downstream of the E1-binding site (*ori* X/X/11), the region downstream of the E1-binding site is now preferentially reactive. Compare *lanes 19* and *23* where the fraction of probe bound was similar. $KMnO_4$ reactivity is barely detectable over the A/T-rich region in the products generated by E2 (*lane 23*), but similar reactivity is observed in the region adjacent to the E2-binding site.

These results imply that the *ori* melting complex is modular in nature, and at least three related species may exist within a spectrum of complexes. One forms at high E1 concentration and melts the DNA symmetrically about the E1-binding site. We have termed this complex *E1*-*ori*. Two others form at low E1 concentration, contain E2, and melt the DNA asymmetrically depending on the position of the distal E2-binding site (*E1-*ori* formed on probe 11/X/X or E1*-*ori* on probe X/X/11). At

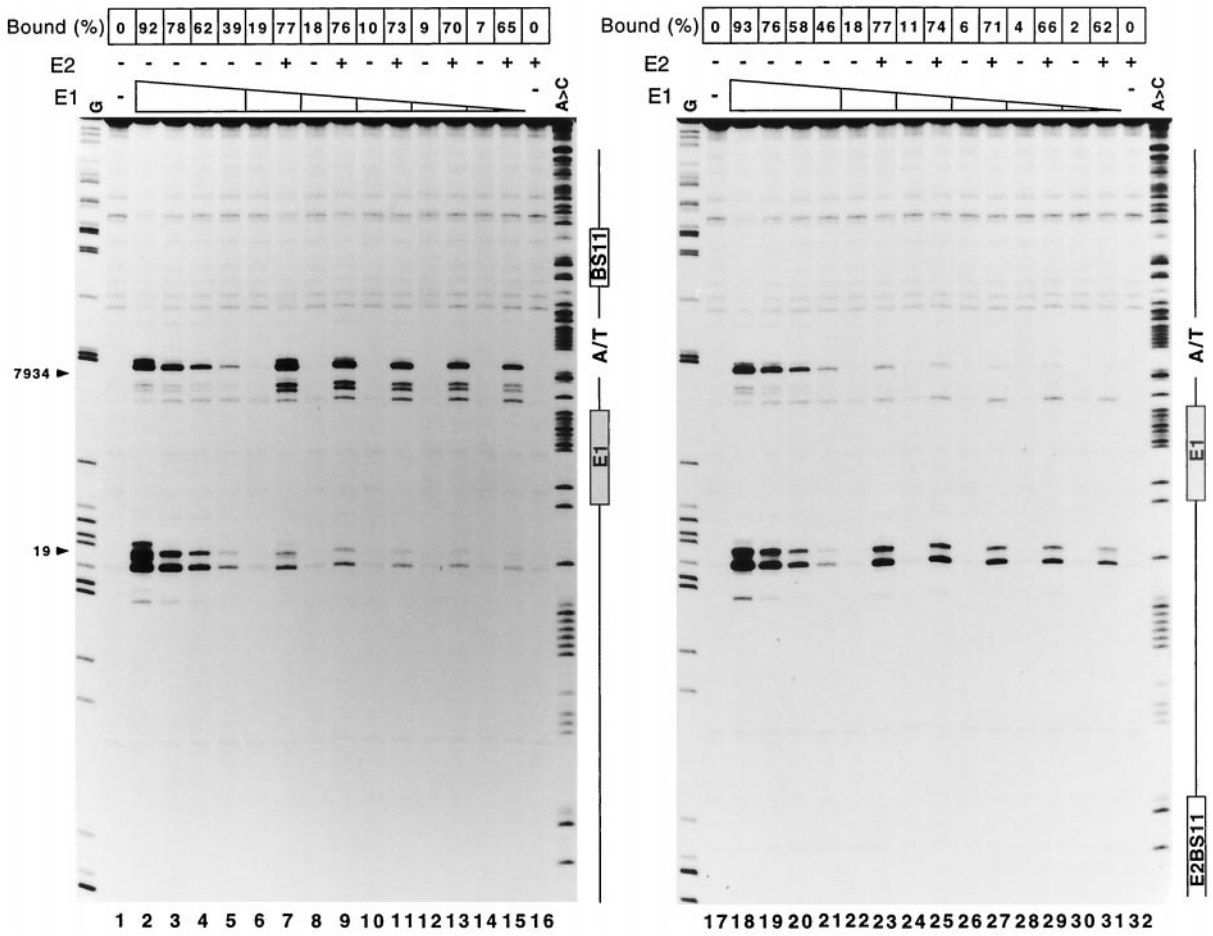

FIG. 4. **Asymmetric melting of *ori* on probes 11/X/X (*left*) and X/X/11 (*right*), *bottom strand* labeled.** Where added, E2 was at 0.625 nM. *Lane 1*, reactivity of free probe. *Lanes 2–5*, E1 at 42.5, 25, 20, and 15 nM. *Lanes 6* and *7*, 10 nM E1; *lanes 8* and *9*, 7.5 nM E1; *lanes 10* and *11*, 5 nM E1; *lanes 12* and *13,* 3.75 nM E1; and *lanes 14* and *15*, 2.5 nM E1. *Lanes 17–32* were as *lanes 1–16.* The faint band migrating slightly above the positions of major reactivity are modified residues where the piperidine reaction has failed to go to completion.

protein concentrations less than those required to form *E1*-*ori,* a population of E1 complexes exists, with various numbers of E1 molecules bound in different configurations. *E1-*ori* and E1*-*ori* would define the minimal complexes that melt upstream or downstream of the E1-binding site. It is possible that more than one complex has this activity but differs in the configuration or number of E1 molecules they contain. E1-*ori* is the complex with little or no melting activity and is operationally defined as the first stable E1 origin complex that can be detected. This complex is also the immediate product of the loading cycle from E2 BS12.

Association of E2 with the E1-ori Complex Is Not Required for Ori Melting—E2 may act simply as a loading factor but could also contribute directly to melting activity. To distinguish between these possibilities, an *ori* melting complex was formed with E2 on a probe with low affinity BS12 at the distal BS11 position and a second low affinity site, E2 BS16 (17), 33 bp downstream of the E1-binding site *ori* 12/X/16 (Fig. 5*A,* E1-binding site represented by the *arrows*). BS12 in the downstream context functions poorly due to its low affinity for E2 but BS16 functions similarly to upstream BS12 (not shown). By using these two E2 sites we might expect to load a full complex that melts the origin symmetrically. Also, on this origin E1-*ori* formation is more efficient at low E2 concentrations (compared with probes with one low affinity E2 site), and E2 dissociates rapidly from the complex. We then challenged reactions with excess oligonucleotide with tandem high affinity E2-binding sites (BS10), and we asked if a change in melting activity accompanied dissociation of E2 from the complex. At various times, samples were processed for gel shift, DNase I footprinting, and the $KMnO_4$ assay (Fig. 5). This allowed us to probe E2 protein-protein and protein-DNA interactions and *ori* melting.

A second probe with only BS12 at the proximal position (X/12/X) was included at equimolar concentration in the reactions as an internal control to ensure that the conditions were only those that would generate the *ori* unwinding complex when E2 loads E1 from a distal binding site. The test template 12/X/16 is 13 bp shorter than the internal control and lacks an *Eco*RI restriction site in the pUC polylinker (Fig. 5*A*). Therefore, in $KMnO_4$ assays, reaction products of the two probes can be differentiated by electrophoretic mobility. For gel shift assays, the ^{32}P label can be cleaved from probe X/12/X with *Eco*RI, so binding products are no longer visible. Also, probe 12/X/16 was biotinylated at one end, allowing selective recovery of this probe on streptavidin-agarose and clear DNase I footprinting of the test template.

Fig. 5*A, lanes 1–9,* shows a gel shift of experimental and control binding reactions after 50 min incubation, cross-linking, and cleavage with *Eco*RI. *Lane 1* is free probe with the small cleavage product of probe X/12/X migrating ahead of the test probe. Reactions in *lanes 2–4* received E1 only, and in *lane 5* the *E1*-*ori* complex was formed by E2 (E2/*E1*-*ori*). E2 binding alone cannot be detected in this assay at low or high E2 concentration (*lanes 6* and *7*). Formation of E2/*E1*-*ori* was inhibited by excess oligonucleotide BS10 (*lane 8*) but not a mutant E2 sequence (*lane 9*). *Lanes 10–21* show a time course

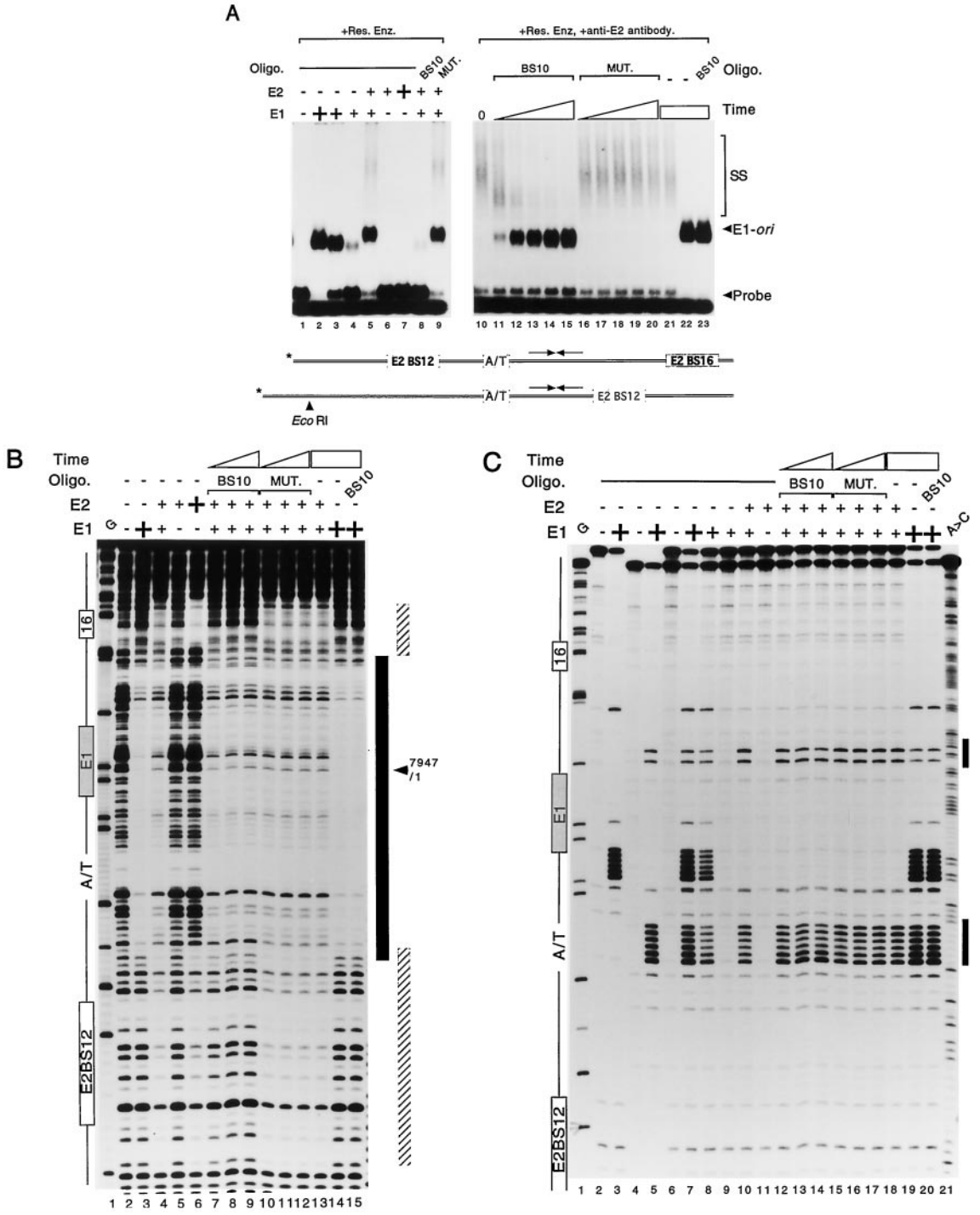

FIG. 5. **E2 is not required for *ori* melting.** Probe 12/X/16 (biotinylated) and X/12/X were mixed at 0.025 nM each. The probes can be differentiated on the basis of size, presence/absence of a restriction site, and streptavidin binding. Reactions were analyzed after 50 min by gel shift, DNase I footprinting, and $KMnO_4$ assays. The reaction where E2 stimulated formation of *E1*-*ori* (E2/*E1*-*ori*) was analyzed further after challenge with specific or nonspecific E2-binding site oligonucleotides (180 nM). *A,* gel shift analysis. *Lanes 1–9* reaction products cross-linked and cut with *Eco*RI after 50 min incubation. *Eco*RI cleaves the probe X/12/X but not 12/X/16, generating a fast migrating product, so only the products of the 12/X/16 binding reaction are observed. *Lane 1*, free probe. *Lane 2–4*, 42.5, 22.5, and 8.75 nM E1. *Lane 5*, E2/*E1*-*ori* complex formed by E2; 8.75 nM E1 and 1.5 nM E2. With this probe, some of the complex migrates with anomalous low mobility. *Lanes 6* and *7*, 1.5 and 1000 nM E2. E2-dependent E1-*ori* complex formation was inhibited by an excess (180 nM) of E2 oligo BS10 (*lane 8*) but not a mutant sequence (*lane 9*). The products of reaction 5 (*lane 5*) were supershifted by anti-E2 antibody (*lane 10*). When challenged with oligo BS10, dissociation of E2 from the complex was observed (T = 50 + 2, 8, 14, 20, and 30 min; *lanes 11–15*) but not on addition of the mutant sequence (same times, *lanes 16–20*) or buffer (*lane 21*). The *E1*-*ori* complex formed at high E1 concentration was unaffected by time (*lane 22*, T = 50 + 20 min), or addition of oligonucleotide (*lane 23*, T = 50 + 20 min). *B,* DNase I footprinting. Probe 12/X/16 was recovered by binding to streptavidin-agarose. *Lane 1*, G ladder. *Lane 2*, cleavage ladder of free probe. *Lane 3*, footprint of *E1*-*ori* formed at high E1 concentration (indicated by the *black bar* to *right*). *Lane 4*, *E1*-*ori* complex formed with E2 (E2/*E1*-*ori*). E2 binding was observed at high (1 μM) but not low (1.5 nM) concentration (*lanes 5* and *6*). *Lanes 7–9*, dissociation of E2 from E2/*E1*-*ori* is observed upon challenge with E2 competitor (T = 50 + 5, 10, and 20 min) but not nonspecific oligo (*lanes 10–12*, same times) or buffer (*lane 13*, T = 50 + 20 min). The footprint of *E1*-*ori* formed at high E1 concentration does not change with time or addition of oligonucleotide (*lanes 14* and *15*). *C,* $KMnO_4$ assay. *Lanes 2* and *3* and *4* and *5* identify the hyper-reactive T residues for the probes X/12/X and 12/X/16 respectively; probes were otherwise mixed. *Lane 6*, reactivity of free probes. *Lanes 7–9*, melting with E1 alone is

after the products of reaction 5 (*lane 5*) were divided and challenged with competitor oligonucleotides or buffer. All samples were cleaved with *Eco*RI and analyzed with anti-E2 antibody. At $T = 50$ min (*lane 10*), anti-E2 antibody supershifted all the complex. Dissociation of E2 could be observed in reactions challenged with BS10 ($T = 50 + 2$, 8, 14, 20, and 30 min; *lanes 11–15*) but not in reactions challenged with mutant oligonucleotide (same times, *lanes 16–20*) or buffer ($T = 50 + 20$ min, *lane 21*). After 20 min challenge with BS10, only 23% of the complex could be supershifted. This decreased to 16% after 30 min and changes little thereafter (not shown). The products of reactions containing a high concentration of E1 were unaffected by time or addition of oligonucleotide BS10 (*lanes 22* and *23*).

Analysis with DNase I is shown in Fig. 5*B*. The footprint of the *E1*-*ori* complex formed at high E1 concentration (*lane 3*) covers approximately 72 bases (*black bar* to the right; BPV nucleotides 7915–39). The E2/*E1*-*ori* complex footprint encompasses the *E1*-*ori* footprint but extends 20–22 nucleotides over both E2-binding sites (*lane 4*). E2 does not bind the probe at low concentration (*lane 5*), but both sites are protected (~23 bases, *hatched bars to right*) at high concentration (*lane 6*). *Lanes 7–9* show a time course of dissociation of E2 from E2/*E1*-*ori* ($T = 50 + 5$, 10, and 20 min) after challenge with BS10. By $T = 50 + 20$ min, binding of E2 to BS12 was undetectable (*lane 9*), but 13% of the probe was protected over BS16. Nonspecific oligonucleotide competitor (or buffer) does not compete with E2 binding to the probe (*lanes 10-13*). The footprint of *E1*-*ori* does not change significantly with time or with addition of oligonucleotide (*lanes 14* and *15*).

Fig. 5*C* shows the results of $KMnO_4$ assays performed under conditions where a high proportion of the probe can be modified. *Lanes 3* and *5* identify the cleavage products of *E1*-*ori* for probes X/12/X and 12/X/16, respectively. *Lane 6* is the reactivity of the mixed free probes. Melting of *ori* at high E1 concentration is observed for both probes (*lanes 7–9*). In *lane 10*, only the complex formed with E2 on probe 12/X/16 was active for origin melting (E2/*E1*-*ori*), with melting of both sides of the E1-binding site (*black bars, right*). Importantly, since no *ori* melting of control probe X/12/X can be detected, most active complexes formed on probe 12/X/16 must have been generated by an E2-dependent mechanism. E2 alone does not induce $KMnO_4$ hyper-reactivity (*lane 11*).

Lanes 12–14 show a time course of $KMnO_4$ reactivity ($T = 50 + 5$, 10, and 20 min) after challenge with E2 competitor. After 20 min challenge, where little or no association of E2 with the complex can be detected (Fig. 5, *A* and *B*), there was no reduction in $KMnO_4$ reactivity over the A/T-rich region compared with control reactions (*lanes 15–17*). However, residues downstream of the E1-binding site, proximal to BS16, are less reactive (24% reduction). Mutation of the natural E2 BS12 sequence adjacent to the E1 site may adversely affect E1 binding in this region and account for this observation. In reactions challenged with buffer (*lanes 18* and *19*), there is a modest increase in $KMnO_4$ reactivity with time, notably over the A/T-rich region. $KMnO_4$ reactivity of *E1*-*ori* formed at high E1 concentration is unaffected by the addition of oligonucleotide (*lane 20*). In conclusion, E2 loads E1 onto the origin from distal binding sites to generate a complex active for origin melting. E2 is free to dissociate from its binding site and is not required to maintain *ori* melting. E2 may, however, contribute to the stability of the complex.

Intermediates in Ori Melting Complex Formation Revealed by Hydroxyl Radical Footprinting—To determine the composition of the various E1 complexes at high resolution, we performed hydroxyl radical footprinting on native complexes. By carefully adjusting the concentrations of E1 and E2 in binding reactions, we were able to favor formation of a desired complex. For example, to analyze E1-*ori*, the concentration of E1 was very low, and complex formation was stimulated by E2 on probe X/12/X to provide adequate complex for analysis. Likewise, the *ori* melting complex *E1*-*ori* was generated at high E1 concentrations where all the probe is bound, and *ori* melting is maximal. Figs. 2 and 4 adequately demonstrate that it is possible to manipulate the reaction conditions to greatly favor formation of the minimal complex with a particular activity. At all but the highest concentrations of E1, where *E1*-*ori* forms, reactions contain excess free probe. To footprint E1-*ori* and other complexes, we derived the scheme shown in Fig. 6*A*. Probes were labeled at one end with ^{32}P and at the other with biotin. Complexes were formed in standard buffer and bound to streptavidin-agarose. If appropriate, reactions were treated with EtBr to dissociate the E1E2-*ori* complex. All reactions were treated with a restriction enzyme that cleaves in the E1-binding site (*Mse*I) and releases a labeled fragment of free probe. Complexes were then washed to remove glycerol and treated with the hydroxyl radical.

In Fig. 6*B*, E2 bound to high affinity BS9 (at the native BS12 position) protected 24 bases on the bottom strand from DNase I cleavage (*lane 2* compared with *3*, *hatched box* to *left*). Three strong hydroxyl radical protections of 5–7 bases each (*I–III*, *black bars, left*) are found within this region (*lanes 4* and *5*). A similar set of hydroxyl radical protection is seen on the top strand (*lane 8* compared with *9*), also within a 24-base DNase I protection (*lanes 6* and *7*). The location of theses protections is shown on the origin sequence in Fig. 6*D*. For each complex, protections are labeled numerically, 5′ to 3′, on both top and bottom strands.

Hydroxyl radical footprints of origin complexes isolated on streptavidin-agarose are shown in Fig. 6*C*. *Lanes 2* and *7* are the cleavage ladders of free probe in the absence and presence of ATP/Mg^{2+} (*top strand*). Six similar sets of protections are seen for the E1E2-*ori* complex formed without (*lane 3*) and with (*lane 4*) ATP/Mg^{2+} (1–6 on the *right* of the panel and Fig. 6*D*) on probe X/12/X. Protections 4–6 over the E2-binding sites are practically identical to I–III generated by E2 binding. Two strong and one weak set of protections are found over and beyond the E1-binding site (protections 1–3), and assuming that there are no radical changes in the way that E2 interacts with DNA in the E1E2-*ori* complex, they are likely those of the E1 dimer. Since binding of a monomer or dimer of E1 cannot be detected in solution (13), this is the only way in which the dimer protection can be determined. As described previously, these strong protections lie predominantly on one face of the DNA helix (11). The dark band in the center of the footprint corresponds to the restriction enzyme cleavage product of the probe. Masked detail in this region was generated separately using a second probe and an enzyme that cuts in the E2-binding site (data not shown). Similar protections were observed on the bottom strand (*lanes 14* and *15*). However, weak

similar for each probe. *Lane 10*, *ori* melting is only observed on probe 12/X/16 when E2 stimulates complex formation. *Lane 11*, E2 does not induce T hyper-reactivity. $KMnO_4$ reactivity changes little over 20 min regardless of challenge with specific competitor (*lanes 12–14*, $T = 50 + 5$, 10, and 20 min), nonspecific competitor (*lanes 15–17*, same times) of buffer (*lane 18*, $T = 50 + 20$ min). $KMnO_4$ reactivity of *E1*-*ori* formed at high E1 concentration, increases slightly with time (*lane 19*), and is unaffected by addition of oligonucleotide (*lane 20*). The annotation on the *left* gives the position of 12/X/16 *ori* sequences, the hyper-reactive Ts are indicated on the *right*.

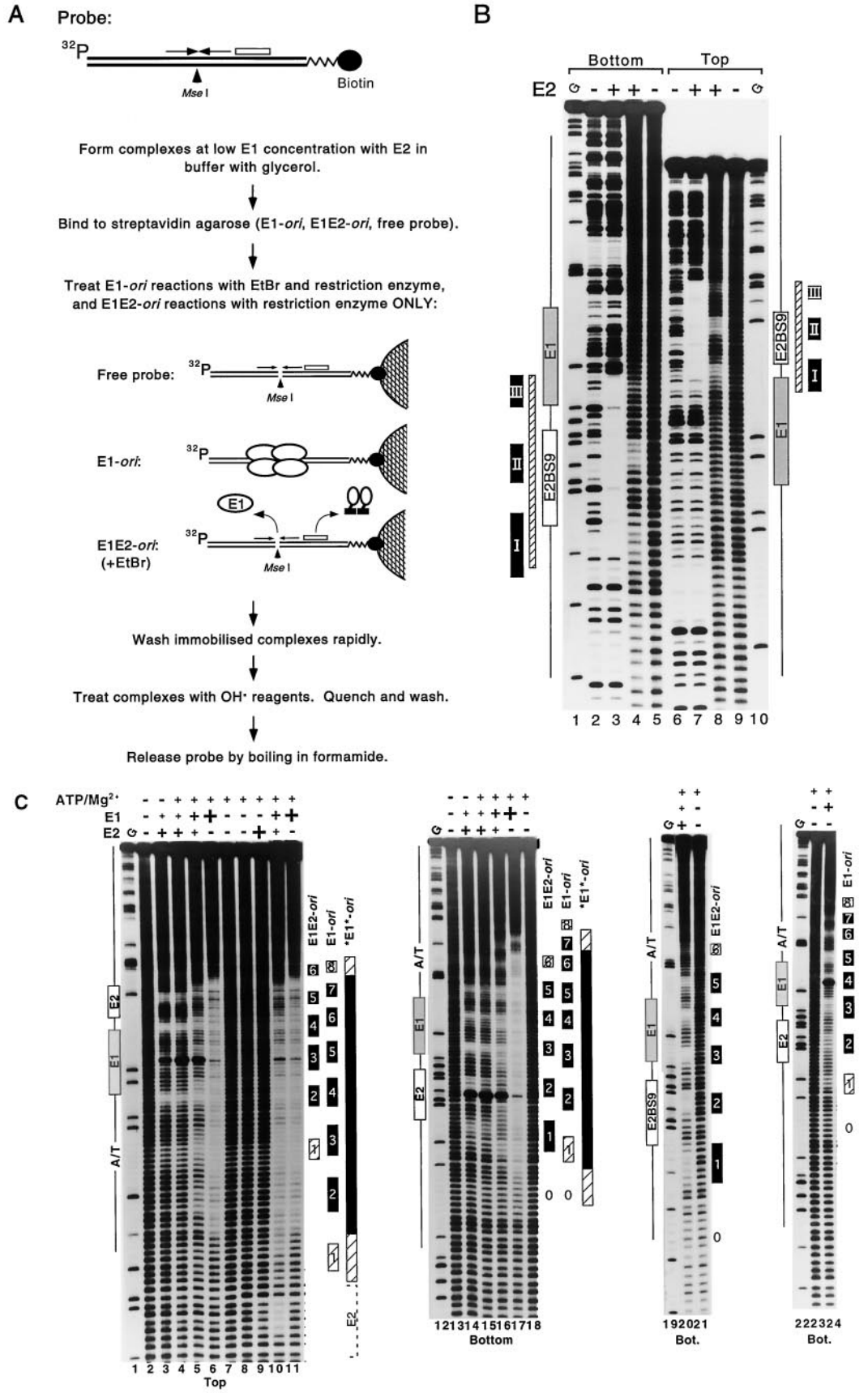

FIG. 6. **Hydroxyl radical footprinting of origin complexes.** *A,* footprinting origin complexes immobilized on streptavidin beads. Note, free probe is released from the beads by cleavage at the *Mse*I site, which is otherwise protected in protein-DNA complexes. Where E2 stimulates E1-*ori* formation, the E1E2-*ori* complex is selectively dissociated with EtBr. *B,* solution footprints of E2. High affinity E2 site BS9 was used since low affinity E2 BS12 proved difficult to footprint. *Lanes 1–5*, *bottom strand*; *lanes 6–10*, *top strand*. *Lanes 1* and *10* are G ladders. *Lanes 2* and *3* and *6* and *7* show the DNase I footprint of an E2 dimer bound to DNA (800 nM E2). Within each DNase I footprint (*hatched boxes*) there are 3 sets of hydroxyl radical protections, *I–III*, *black boxes. C,* hydroxyl radical footprints of E1E2-*ori* and E1-origin complexes immobilized on streptavidin-

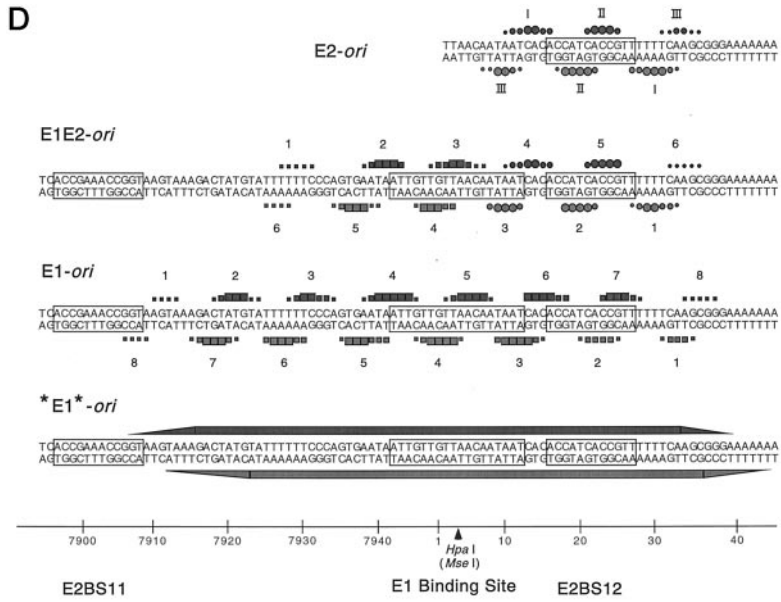

FIG. 6—*continued*

protection 6 (*bottom strand*) was only clear in the complex formed on a probe with high affinity E2 BS9 (*lane 20*), where all protections are stronger.

In E1-*ori* generated by E2 in the presence of ATP/Mg^{2+} on probe X/12/X (Fig. 6*C*, *lanes 5, top strand,* and *16* and *24*, *bottom strand*), there are similar protections on both strands. Within a general protection of approximately 75 bases, there are six sets of strong protections (protections 2–7), flanked by two weaker sets (protections 1 and 8), as indicated on the *right* and in Fig. 6*D*. Protections 4 and 5 on each strand are related to the strong protections of the E1 dimer in the E1E2-*ori* complex. The repeated protections on either side of these are best interpreted as the binding of two additional E1 dimers. Contacts generating the weak E1 protections in E1E2-*ori* (protections 1 and 6, *top* and *bottom strand*, respectively) may no longer occur upon binding of additional dimers but are formed by these dimers at related positions in E1-*ori* (protections 1 and 8, *top* and *bottom strand*). Therefore, in E1-*ori* six E1 monomers contact the DNA. The strong protections of each additional E1 dimer lie predominantly on the same face of the helix as those of the first E1 dimer deposited by E2. However, the general protection within the region suggests that the protein wraps extensively around the DNA, since this would reduce the rate of hydroxyl radical attack. This is a likely explanation since this is also observed for E1E2-*ori* (*lanes 3, 4, 15,* and *20*), formed at very low E1 concentrations where complex heterogeneity is likely to be minimal or non-existent, as judged by EtBr sensitivity of the products. In *E1*-*ori*, the DNA is completely protected over 60–65 bases on each strand, with weaker protections tapering at the flanks (*lanes 6* and *17*). Where E2 loads E1 from a distal binding site (probe 11/X/X, *lanes 8–11*), the probe is completely protected in the region adjacent to the distal E2-binding site (*lane 10*), as in *E1*-*ori* (*lane 11*), but the partial protections of E1-*ori* (*lane 5*) are present downstream. This is good evidence that E1-*ori* is a sub-complex of *E1*-*ori*. Similar results were obtained for both strands and when the E2-binding site is moved to a distal position downstream of the E1-binding site (data not shown).

Our data are consistent with stepwise loading of E1 to generate the *ori* melting complex and with the idea that E2 serves to assemble complexes at limiting E1 concentrations. The E2-dependent loading cycle from proximal E2 BS12 deposits six E1 molecules on the DNA, generating E1-*ori*. This complex is stable, has *ori* specificity (imparted to a significant degree by E2), and the DNA lies on a protein surface generated by E1 multimerization. E1-*ori* is likely to be the core of a higher order origin melting complex, *E1*-*ori*. Two subdomains of this complex, which share the E1-*ori* core, function independently to melt the DNA on either side of the E1-binding site.

Modular Assembly of the E1-ori Melting Complex—The asymmetric *ori* melting observed with E2 at the distal position (Fig. 4) indicated that symmetrical melting in *E1*-*ori* is achieved through the action of two distinct units. We therefore asked whether the *ori* DNA could be melted on a probe truncated immediately downstream of the E1-binding site. On such a probe, we would not expect to form the complete E1-*ori*

agarose. E1E2-*ori* (*lanes 3, 4, 14, 15,* and *20*), 3 nM E1 and 3.5 nM E2; E1-*ori* (*lanes 5, 16,* and *24*), 7.5 nM E1 and 0.75 nM E2; *E1*-*ori* (*lanes 6, 11,* and *17*), 60 nM E1. The probe used was X/12/X except *lanes 8–11* where probe 11/X/X was used, and *lanes 20* and *21* which show the E1E2-*ori* complex formed on a probe with high affinity E2 BS9. The footprints of E1E2-*ori* were similar regardless of the presence of ATP/Mg^{2+} (compare *lanes 3* and *4* and *14* and *15*) or the E2-binding site sequence (*lane 21*, E2 BS9). Periodic sets of protections were observed for E1E2-*ori* and E1-*ori*; stronger protections are shown as *black boxes* and weaker protections as *hatched boxes* (*right*). A single very weak set of protections (*0*) is also observed on the *bottom strand* only, downstream of the E2 site and protection 1 in E1E2-*ori* and E1-*ori*. It is sequence-independent and appears to be unrelated to the other periodic protections. *E1*-*ori* gave rise to a large block protection with weaker protections tapering at the flanks (*lanes 6, 11,* and *17*). In *lanes 8–11* the probe was 11/12/X. *Lane 8* is free probe. *Lane 9* shows a weak E2 footprint on BS11 (1250 nM E2). In *lane 10*, E1 complex formation was stimulated by E2 (7.5 nM E1 and 0.75 nM E2). The region adjacent to the E2-binding site is completely protected, but the protections downstream of the E1-binding site resemble those of E1-*ori* (*lane 5*). The strong band in the center of the E1-binding site in *lanes 3–5* corresponds to the restriction enzyme (*Mse*I) cleavage product. To obtain details in this region, complexes were also formed and footprinted on a probe with a *Hae*III restriction site in the nonconserved core sequence of the E2 BS12-binding site. Results for this probe are shown for the *bottom strand* (*lanes 12–18*) and are compared with the regular probe, *lanes 23* and *24. D,* location of hydroxyl radical protections. The size of each *circle* (E2 protections) or *square* (E1 protection) is an estimate of the degree of protection determined from analysis of several autoradiographs. The E2 footprint is clearly recognizable in the E1E2-*ori* complex. The protections in E1-*ori* can be interpreted as the binding of six molecules of E1 to the DNA. In *E1*-*ori*, more than 70 bases are protected on each strand, with weaker protections at the flanks.

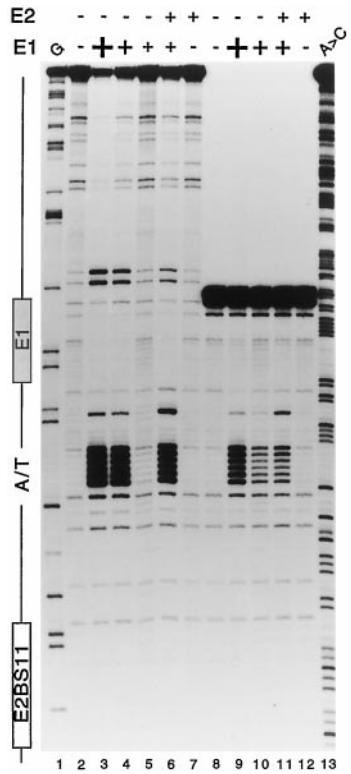

FIG. 7. **Melting of a truncated origin probe.** A truncated probe with distal E2 BS11 was generated using a primer terminating immediately downstream of the E1-binding site. This was analyzed in parallel with full-length probe 11/X/X. *Lane 1,* G ladder. *Lanes 2–7*, full-length probe 11/X/X. *Lane 2,* free probe. *Lanes 3* and *4*, 60 and 47.5 nM E1 only. *Lanes 5* and *6*, 10 nM E1 without and with (*lane 6*) E2 (1 nM). *Lane 7*, E2 (1 nM). *Lanes 8–12,* truncated probe. *Lane 8*, free probe. *Lane 9*, 60 nM E1, required for complete site occupancy. *Lanes 10* and *11*, 47.5 nM E1, without and with (*lane 11*) E2. *Lane 12*, E2 alone, 1 nM. Origin melting occurred on the truncated probe at high E1 concentration (*lane 9*) and when E2 stimulated complex formation (*lane 11*).

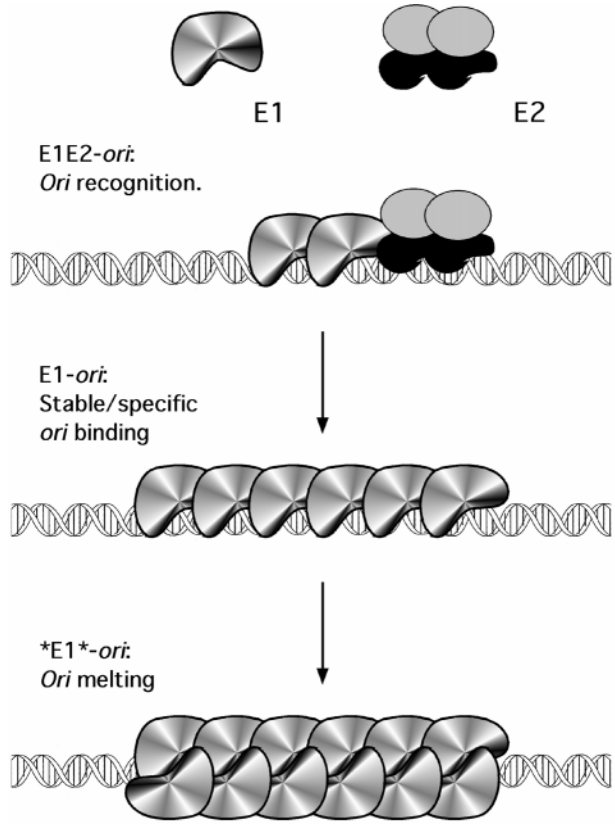

FIG. 8. **Origin complex assembly.** Specific *ori* recognition is by the E1E2-*ori* complex. Two E1 monomers are first recruited to the E1-binding site by E2 bound to proximal BS12 or from distal binding sites.[2] In E1-*ori*, the first stable *ori*-specific E1 complex that forms, three E1 dimers contact one face of the DNA helix. The melting complex *E1*-*ori* forms from E1-*ori*. E2 bound to distal sites can recruit E1 to E1-*ori* lowering the concentration of E1 required for *ori* melting. The DNA is completely protected from hydroxyl radical attack over about 70 base pairs, and the DNA is melted either side of the E1-binding site. This may correspond to the bi-lobed structure observed by EM (20). Two units are active for DNA melting in this complex, although they form through a common precursor.

complex. Binding reactions were analyzed with the $KMnO_4$ assay (Fig. 7) and also by gel shift and DNase I footprinting (not shown). Without E2, E1 bound the truncated probe, but about 50% more protein was required for full site occupancy. E2 also stimulated complex formation on the truncated probe with upstream BS11. In each case, complexes formed on the full-length and truncated probes shared the same upstream boundaries, as determined by DNase I footprint analysis. Cross-linked complexes were stable in the presence of EtBr and could be supershifted with anti-E2 antibody (data not shown).

As expected, the *ori* DNA was melted on the full-length probe when *E1*-*ori* was formed at high E1 concentration (Fig. 7, *lanes 3* and *4*) or at low E1 concentration with E2 (*lane 6*). For the truncated probe, the *ori* DNA was also melted at high E1 concentration but at a reduced extent compared with the full-length probe (*lane 9* compared with *3*). All the same T residues were hyper-reactive, with no additional modifications. Origin melting was also detectable for the complex formed in the presence of E2 (*lane 11*). Similar results were obtained for the other strand or for probes with downstream sequences, truncated upstream of the E1-binding site. Therefore, sequences including those that bind E1 molecules in the sub-complex E1-*ori* are not required for formation of an *ori* melting complex. *E1*-*ori* may be composed of two functional units on each half of the origin that form through a common precursor, E1-*ori*. They may cooperate in *ori* melting, possibly by reciprocal stabilization.

DISCUSSION

Stepwise Formation of the BPV-1 Origin Melting Complex—A model for assembly of the *ori* melting complex is shown in Fig. 8. A dimer of E1 is first recruited to the E1-binding site by cooperative interactions with E2 bound to proximal E2 BS12 (13) or distal BS11.[2] Sequences in the E1 palindrome are critical for dimer binding. In the first E1 complex that forms on the origin (E1-*ori*), E1 binds DNA as a trimer of dimers (Fig. 6). The highly cooperative nature of E1 complex formation suggests that E1 protein-protein interactions are important for binding of additional molecules. However, the first E1 dimer could also alter the structure of the flanking DNA in a subtle fashion, favoring E1 binding. Hydrolyzable ATP is important for complex formation. Without a hydrolyzable nucleotide, the only E1 complex that forms on the origin also contains six E1 molecules (20), which contact the DNA, but is some 5-fold less stable (7).[2] ATP/Mg^{2+} could induce conformational changes in E1 that stabilize E1-E1 interactions, contacts with DNA, or both.

The origin melting complex, *E1*-*ori*, forms from E1-*ori*. Addition of E1 molecules and ATP/Mg^{2+} are critical for the transition. As the DNA backbone is completely protected, the number of E1 molecules contacting DNA in *E1*-*ori* cannot be deduced. However, a bi-lobed structure believed to correspond to a double hexamer of E1 encircling the origin has been observed by EM (20). This forms under similar conditions, and the length (125 Å) would encompass DNA similar in size to our

nuclease protections. T-antigen forms a similar structure (21, 22). The additional molecules that contact DNA may bind opposite the original six molecules in E1-*ori* that make strong contacts on one face of the helix.

The proposed E1 and T-antigen initiator assembly pathways are similar, but there are also some important differences between the two models. Four pentanucleotide T-antigen-binding sites (sites 1–4) in the center of the SV40 core *ori* divide the origin into early and late halves and bind four T-antigen monomers in the absence of ATP (23). In the presence of ATP, T-antigen binds pentanucleotide 1 and then 2, nucleating assembly of a hexamer on the early half of the origin. The early hexamer then enhances the assembly of a second hexamer on the late half of the origin, melting the early and late DNA (21). For *E1*-*ori*, complex formation is also guided by the E1-binding site, but without any additional factors, there is little evidence for asymmetric complex assembly. Thus, two T-antigen hexamers assemble sequentially, but the equivalent E1 structures assemble coordinately. Also, T-antigen and E1 differ in their nucleotide requirement for complex formation and DNA melting. DNA melting by T-antigen does not require a hydrolyzable cofactor (3, 24, 25) but E1 does (14). Unlike the lytic SV40 virus, replication of BPV-1 is cell cycle-regulated (26). The requirement for ATP for complex formation and melting by E1 may provide an opportunity for regulation by control of ATP binding or hydrolysis.

Loading of E1 by E2—E2 confers specificity and affinity on E1 binding, loading the origin from proximal (E2 BS12) or distal (BS11) E2 sites. However, the immediate product of the loading cycle from BS12, E1-*ori,* is inactive for *ori* melting. It is likely that a second E1 dimer is first recruited over the A/T-rich region, and E2 is displaced before the third dimer binds. With a distal E2-binding site, E1-*ori* also appears to form through the same sequence of events, although in this case, the second E1 dimer may bind downstream of the E1-binding site (Fig. 6*C*).[2] Without steric constraints, E2 promotes formation of the *E1*-*ori* melting complex, most likely by loading more E1 molecules. E2 therefore appears to act generally as a specificity factor, obligatory for generating stable and specific E1 binding, but also promotes the transition in *ori* complex activity by recruiting additional E1 molecules. The activity of E2 BS11 may result in preferential melting of the DNA upstream of the E1-binding site. However, this asymmetric loading of E1 does appear to facilitate E1 binding downstream of the E1-binding site, and this could be assisted further by E2 bound elsewhere.

Our data suggest that proximal E2 BS12 is redundant, since distal E2 BS11 alone can drive formation of the *E1*-*ori* complex more efficiently *in vitro*. One question is the relevance of the proximal E2 site, which is conserved in the fibropapillomaviruses. E2 is bound stably to BS12 when the E1E2-*ori* complex forms without ATP/Mg^{2+}. This complex is inhibitory for E1-*ori* formation (7) and could govern its formation if ATP binding or hydrolysis by E1 were regulated. Although this has not been demonstrated, E1E2-*ori* formed without a hydrolyzable nucleotide appears well oriented toward this role. The complex forms with high affinity and also appears to actively prevent recruitment of additional E1 molecules to the DNA (7). Binding of E1 downstream of the E1-binding site is blocked directly by E2 binding (Fig. 6*C*). Binding over the A/T-rich region could be prevented if appropriate protein-protein interactions cannot occur or if the DNA adopts an unfavorable conformation. E1 interacts with both the E2 activation (AD) and DNA-binding domains (DBD) when binding sites are close (as BS12) but only the AD when sites are at a distance (27). The E1-E2 DBD interaction could be the critical component of ATP-dependent regulation. Regulating ATP binding or hydrolysis to control initiation has been suggested for *Escherichia coli* DnaA (28) and the origin recognition complex of yeast (29). BS12 can clearly fulfill the role of E2 that is necessary for replication, but how the transition to the *ori* melting complex occurs without a distal E2-binding site is unclear. *In vivo*, this could be simply dependent on E1 concentration.

Structure of E1-ori, the Origin Melting Complex and Transition to a Mobile Helicase—Although initiator melting reactions share some requirements, such as multiple DNA-binding sites and regions of low thermodynamic stability, there appears to be no clearly conserved mechanism. Initiators either loop, wrap, or encircle the DNA to melt the appropriate region. For example, HSV UL9 protein binds as a dimer to two sites, loops the intervening DNA, and uses the free energy of supercoiling for melting (30). Both λ O and *E. coli* Dna A wrap the DNA on the surface of a large protein complex, melting the DNA in adjacent regions (28, 31, 32). The E1-*ori* complex appears to resemble these complexes, but significant structural changes in the DNA cannot be detected.[2] The six E1 molecules form strong contacts on one face of the helix, suggesting that the DNA lies on a protein surface. However, E1 also wraps extensively around the DNA, since there is a general decrease in the rate of hydroxyl radical attack over the entire region, which also appears inaccessible to the intercalator EtBr. It is unclear whether the DNA is wrapped around a protein core in E1-*ori* or if the protein and DNA are aligned more like two rods. In the λ Osome, four dimers of the O protein bind, bend the DNA successively (33), and wrap the DNA completely around the protein (34). DNA bending at origins of replication, either intrinsic or protein induced, appears to be common, but its significance is unclear. DNA bending may be required for the strand separation reaction. We have observed that E1 is capable of bending DNA,[3] and E1-*ori* may therefore have a role in the strand separation reaction.

In the origin melting complex *E1*-*ori* the DNA is encircled by E1, and EM studies show the DNA tacking a straight path through a complex formed under similar conditions (20). Encirclement appears to be required for melting and is concomitant with formation of the bi-lobed double hexamer. The minimal E1 helicase is a hexamer (20, 35) and belongs to a general class of hexameric ring-like helicases (36). How transition from origin melting complex to mobile helicase occurs has not been addressed, but the available evidence suggests that E1 and T-antigen require only single-stranded-binding protein (SSB) to initiate translocation. Probing with dimethyl sulfate and $KMnO_4$ suggests that in *E1*-*ori* the DNA adjacent to the E1-binding site is melted with few base contacts, but over the E1-binding site the DNA remains double-stranded and makes extensive base contacts with E1.[2] This has also been observed for the analogous T-antigen structure (24). All proposed unwinding mechanisms require the helicase to have at least two DNA-binding sites. If unwinding is by an active mechanism, both single- and double-stranded DNA must be bound simultaneously (36). *E1*-*ori* (and the T-antigen complex) may be helicases paused at the first round of denaturation. Stabilization of the unwound region by SSB may be required so that the energy of ATP hydrolysis is sufficient to couple denaturation with translocation. However, the only single-stranded DNA that can be detected with current probes is protected by protein. The action of SSB therefore remains to be fully explained, as do the mechanisms of DNA melting and unwinding by E1 and helicases in general.

Acknowledgment—We thank James Chong for critical reading of the manuscript.

[3] E. Gillitzer and A. Stenlund, unpublished observations.

REFERENCES

1. Kodadek, T. (1998) *Trends Biochem. Sci.* **23,** 79–83
2. Borowiec, J. A., Dean, F. B., Bullock, P. A., and Hurwitz, J. (1990) *Cell* **60,** 181–184
3. Parson, R., Anderson, M. E., and Tegtmeyer, P. (1990) *J. Virol.* **64,** 509–518
4. Seo, Y.-S., Müller, F., Lusky, M., and Hurwitz, J. (1993) *Proc. Natl. Acad. Sci. U. S. A.* **90,** 702–706
5. Yang, L., Mohr, I., Fouts, E., Lim, D. A., Nohaile, M., and Botchan, M. (1993) *Proc. Natl. Acad. Sci. U. S. A.* **90,** 5086–5090
6. Lusky, M., Hurwitz, J., and Seo, Y.-S. (1994) *Proc. Natl. Acad. Sci. U. S. A.* **91,** 8895–8899
7. Sanders, C. M., and Stenlund, A. (1998) *EMBO J.* **17,** 7044–7055
8. Ustav, M., and Stenlund, A. (1991) *EMBO J.* **10,** 449–457
9. Ustav, E., Ustav, M., Szymanski, P., and Stenlund, A. (1993) *Proc. Natl. Acad. Sci. U. S. A.* **90,** 898–902
10. Sedman, J., and Stenlund, A. (1995) *EMBO J.* **14,** 6218–6228
11. Sedman, J., and Stenlund, A. (1996) *EMBO J.* **15,** 5085–5092
12. Sedman, T., Sedman, J., and Stenlund, A. (1997) *J. Virol.* **71,** 2887–2896
13. Chen, G., and Stenlund, A. (1998) *J. Virol.* **72,** 2567–2576
14. Gillette, T. G., Lusky, M., and Borowiec, J. A. (1994) *Proc. Natl. Acad. Sci. U. S. A.* **91,** 8846–8850
15. Gillette, T. G., and Borowiec, J. A. (1998) *J. Virol.* **72,** 5735–5744
16. Ito, K., Asano, M., Hughes, P., Kohzaki, H., Masutani, C., Hanaoka, F., Kerppola, T., Curran, T., Murakami, Y., and Ito, Y. (1996) *EMBO J.* **15,** 5636–5646
17. Li, R., Knight, J., Bream, G., Stenlund, A., and Botchan, M. R. (1991) *Genes Dev.* **3,** 510–526
18. Dixon, W. J., Hayes, J. J., Levin, J. R., Weidner, M. F., Dombroski, B. A., and Tullius, T. D. (1991) *Methods Enzymol.* **208,** 380–413
19. Sasse-Dwight, S., and Gralla, J. D. (1991) *Methods Enzymol.* **208,** 147–169
20. Fouts, E. T., Yu, X., Egelman, E. H., and Botchan, M. R. (1999) *J. Biol. Chem.* **274,** 4447–4458
21. Parsons, R., Stenger, J. E., Ray, S., Welker, R., Anderson, M. E., and Tegtmeyer, P. (1991) *J. Virol.* **65,** 2798–2806
22. Mastrangelo, I. A., Hough, P. V. C., Wall, J. S., Dodson, M., Dean, F. B., and Hurwitz, J. (1989) *Nature* **338,** 658–662
23. Mastrangelo, I. A., Hough, P. V. C., Wilson, V. G., Wall, J. S., Hainfield, J. F., and Tegtmeyer, P. (1985) *Proc. Natl. Acad. Sci. U. S. A.* **82,** 3626–3630
24. Borowiec, J. A., and Hurwitz, J. (1988a) *EMBO J.* **7,** 3149–3158
25. Borowiec, J. A., and Hurwitz, J. (1988b) *Proc. Natl. Acad. Sci. U. S. A.* **85,** 64–68
26. Ravnan, J.-B., Gilbert, D. M., Ten Hagen, K. G., and Cohen, S. N. (1992) *J. Virol.* **66,** 6946–6952
27. Berg, M., and Stenlund, A. (1997) *J. Virol.* **71,** 3853–3863
28. Bramhill, D., and Kornberg, A. (1988) *Cell* **52,** 743–755
29. Klemm, R. D., Austin, R. J., and Bell, S. P. (1997) *Cell* **88,** 493–502
30. Koff, A., Schwedes, J. F., and Tegtmeyer, P. (1991) *J. Virol.* **65,** 3284–3292
31. Schnos, M., Zahn, K., Inman, R. B., and Blattner, F. R. (1988) *Cell* **52,** 385–395
32. Fuller, R. S., Funnell, B. E., and Kornberg, A. (1984) *Cell* **38,** 889–900
33. Zahn, K., and Blattner, F. R. (1985) *EMBO J.* **13,** 3605–3616
34. Dodson, M., Roberts, J., McMacken, R., and Echols, H. (1985) *Proc. Natl. Acad. Sci. U. S. A.* **82,** 4678–4682
35. Sedman, J., and Stenlund, A. (1998) *J. Virol.* **72,** 6893–6897
36. Lohman, T. M., and Bjornson, K. P. (1996) *Annu. Rev. Biochem.* **65,** 169–214